

Baryon distribution for high energy heavy ion collisions in a Parton Cascade Model

Yasushi Nara

RIKEN BNL Research Center, Brookhaven National Laboratory, Upton, New York, 11973, USA

The baryon distribution is studied by using a parton cascade model which is based on pQCD incorporating hard partonic scattering and dynamical hadronization scheme. In order to study baryon distribution, baryonic cluster formation is newly implemented as well as hadronic higher resonance states from parton/beam cluster decay. The net baryon number and charged hadron distributions are calculated with different K -factors in which parameters are fixed by elementary $p\bar{p}$ data at $E_{c.m.} = 200$ GeV. It is found that baryon stopping behavior at SPS and RHIC energies are not consequence of hard parton scattering but soft processes.

24.85.+p,25.75.-q,13.85,12.38M

I. INTRODUCTION

Heavy ion experiments at BNL-AGS and CERN-SPS have been performed motivating by the possible creation of QCD phase transition and vast body of systematic data such as proton, pion strangeness particles distributions, HBT correlation, flow, dileptons and J/ψ distributions have been accumulated including mass dependence and their excitation functions [1–3]. Data from forthcoming experiment at BNL-RHIC will be available soon.

Strong stopping of nuclei has been reported both at AGS and at SPS energies [4,5]. It is reported that baryon stopping power can be understood within a hadronic models if we consider multiple scattering of nucleon using reasonable pp energy loss [6]. For example, within string based models [7–11], baryon stopping behavior at SPS energies is well explained by introducing diquark breaking mechanism in which diquark sitting at the end of the string breaks. Diquark breaking leads to large rapidity shifts of the baryon. Constituent quark scattering within a formation time [8,12] has to be considered in order to generate Glauber type multiple collision at initial stage of nuclear collisions in microscopic transport models which describe full space-time evolution of particles.

Event generators based on perturbative QCD (pQCD) are proposed such as HIJING (Heavy Ion Jet Interaction Generator) [13,14], VNI (Vincent Le Cucurullo Con Giginello) [15], in order to describe ultra-relativistic heavy ion collisions emphasizing the importance of mini-jet productions. VNI can follow the space-time history of partons and hadrons. The parton cascade model of VNI has been applied to study several aspects of heavy-ion collisions even at SPS energies [17]. However, original version of VNI implicitly assumed the baryon free region at mid-rapidity during the formation of hadrons, because only two parton cluster (mesonic cluster) formations are included in the Monte-Carlo event generator VNI [15].

In this work, The baryon distribution at SPS and RHIC energy are discussed using modified version of parton cascade simulation code VNI [16]. The main features of the parton cascade model to be used here are that implementation of baryonic cluster formation and during the parton/beam cluster decay higher hadronic resonance states are allowed to produce in order to be able to calculate baryon distribution in heavy ion collisions.

II. PARTON CASCADE MODEL

First of all, the main features of the parton cascade model of VNI as well as the main points of the modification will be presented. Relativistic transport equations for partons based on QCD [18] are basic equations which are solved on the computer in parton cascade model. The hadronization mechanism is described in terms of dynamical parton-hadron conversion model of Ellis and Geiger [19–21]. The main features in the Monte Carlo procedure are summarized as follows.

1) The initial longitudinal momenta of the partons are sampled according to the measured nucleon structure function $f(x, Q_0^2)$ with initial resolution scale Q_0 . We take GRV94LO (Lowest order fit) [22] for the nucleon structure function. The primordial transverse momenta of partons are generated according to the Gaussian distribution with mean value of $p_\perp = 0.44$ GeV. The individual nucleons are assigned positions according to a Fermi distribution for nuclei and the positions of partons are distributed around the centers of their mother nucleons with an exponential distribution with a mean square radius of 0.81 fm.

2) With the above construction of the initial state, the parton cascading development proceeds. Parton scattering are simulated using closest distance approach method in which parton-parton two-body collision will take place if their impact parameter becomes less than $\sqrt{\sigma/\pi}$, where σ represents the parton-parton scattering cross section calculated by pQCD within a Born approximation. Both spacelike and timelike radiation corrections are included within the leading logarithmic approximation. Elementary $2 \rightarrow 2$ scatterings, $1 \rightarrow 2$ emissions and $2 \rightarrow 1$ fusions are included in the parton cascading.

3) Parton clusters are formed from secondary partons that have been produced by the hard interaction and parton branching. The probability of the parton coalescence to form color-neutral cluster Π is defined as [20]

$$\Pi_{ij \rightarrow C} = \begin{cases} 0, & L_{ij} \leq L_0, \\ 1 - \exp\left(\frac{L_0 - L_{ij}}{L_c - L_{ij}}\right), & L_0 < L_{ij} \leq L_c, \\ 1, & L_{ij} > L_c, \end{cases} \quad (1)$$

where $L_c = 0.8\text{fm}$ is the value for the confinement length scale and $L_0 = 0.6\text{fm}$ is introduced to account for finite transition region. L_{ij} is defined by the distance between parton i and its nearest neighbor j :

$$L_{ij} \equiv \min(\Delta_{i1}, \dots, \Delta_{ij}, \dots, \Delta_{in}), \quad (2)$$

where $\Delta_{ij} = \sqrt{r_i^\mu r_{j\mu}}$ is the Lorenz-invariant distance between partons. So far, only the following two-parton coalescence

$$g + g \rightarrow C_1 + C_2, g + g \rightarrow C + g, g + g \rightarrow C + g + g, \quad (3)$$

$$q + \bar{q} \rightarrow C_1 + C_2, q + \bar{q} \rightarrow C + g, \quad (4)$$

$$q + g \rightarrow C + q, q + g \rightarrow C + g + q. \quad (5)$$

have been considered in the VNI model. In this work, if diquarks are formed with the above formation probability, baryonic cluster formation is included as

$$qq + q \rightarrow C, \quad (6)$$

$$\bar{q}\bar{q} + \bar{q} \rightarrow C, \quad (7)$$

$$q_1 q_2 + \bar{q}_3 \rightarrow q_1 \bar{q}_3 + q_2, \quad (8)$$

$$q_1 q_2 + g \rightarrow q_1 q_2 q_3 + \bar{q}_3. \quad (9)$$

Note that by introducing those cluster formation processes, We do not introduce any new parameters into the model.

4) Beam clusters are formed from primary partons (remnant partons) which do not interact during the evolution even though they travel in the overlapping region of nuclei. They may be considered as the coherent relics of the original hadron wavefunctions, and should have had soft interactions. Those underlying soft interactions are simulated by the beam cluster decay into hadrons in VNI because additional possibility that several parton pairs undergo soft interactions. This may give a non-negligible contribution to the ‘underlying event structure’ even at the collider energies. The primary partons are grouped together to form a massive beam cluster with its four-momentum given by the sum of the parton momenta and its position given by the 3-vector mean of the partons’ positions.

5) The decay probability density of each parton cluster into final state hadrons including hadronic resonances is chosen to be a Hagedorn density state. The appropriate spin, flavor, and phase-space factors are also taken into account. In the decay of parton/beam cluster, higher hadronic resonance states up to mass of 2GeV can be produced in our model.

To summarize, the main different points from original version are 1) baryonic cluster formation. 2) inclusion of higher hadronic resonance up to mass of 2GeV. 3) exact conservation of flavor, i.e. (baryon number, charge,etc). 4) reasonable total momentum conservation: total momentum is conserved within 10% at RHIC energy for central Au+Au collision.

III. RESULTS

A. Elementary collisions

Since our version of parton cascade code differs from original version of VNI, we have to check the model parameters. First, particle spectra from $p\bar{p}$ collisions at $\sqrt{s} = 200\text{GeV}$ calculated by the modified version of VNI are studied to

see the model parameter dependence. Here we see the K -factor dependence as mentioned in Ref. [23]. In Fig. 1, experimental data on pseudorapidity distributions (left panel) and the invariant cross sections (right panel) are compared to the calculation of the parton cascade model with different parameters on the treatment of so-called K -factor. The calculations (upper three figures) are done by adding the constant factor to the reading-order pQCD cross sections:

$$\sigma_{pQCD}(Q^2) = K \times \sigma^{LO}(Q^2)$$

with values $K = 1, 2, 2.5$. While bottom figure corresponds to the calculation changing the Q^2 scale in the running coupling constant α_s as

$$\sigma_{pQCD}(Q^2) = \sigma^{LO}(\alpha_s(\eta Q^2))$$

with the value $\eta = 0.075$. We also plot the contribution from parton cluster decay in the left panel with dotted lines. The contribution of parton cluster decay which is come from interacted parton coalescence changes according to the choice of the correction scheme. We can fit the $p\bar{p}$ data of pseudorapidity distributions with different correction schemes as seen in Fig. 1 by changing the parameter (in actual code, `parv(91)`) which controls the multiplicity from beam cluster. We have to check the model with various elementary data including incident energy dependence in order to fix model parameters. Next we will present some results on nuclear collisions with those parameters.

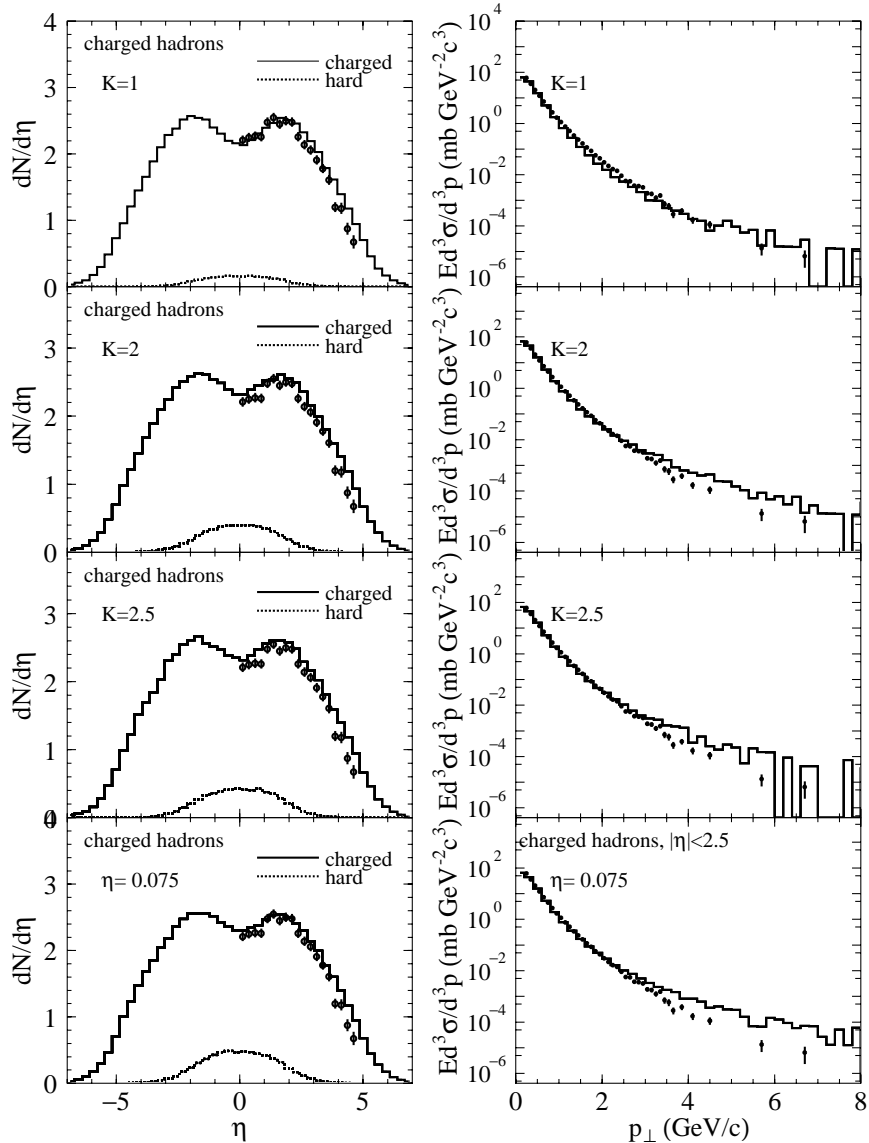


FIG. 1. Data on charged particle ($(h^- + h^+)/2$) pseudorapidity (left) [24] and the invariant cross sections $Ed^3\sigma/d^3p$ (right) [25] from $p\bar{p}$ collision at $\sqrt{s} = 200\text{GeV}$ compared to parton cascade model calculations with various parameters. The contributions from parton cluster decay are also plotted by dotted lines in a left panel.

B. Comparison with SPS data

The baryon stopping problem is one of the important element in nucleus-nucleus collisions. Original version of VNI implicitly assumed baryon free region at midrapidity, because baryonic parton cluster formation is not included. Baryons only come from beam cluster, not parton cluster formation in the original version of VNI. We can now discuss the baryon stopping problem with our modified version of VNI.

We have calculated the net proton distribution at SPS energy to show the reliability of the modeling of beam cluster formation in the parton cascade model. Fig. 2 compares the parton cascade calculation for $\text{Pb}+\text{Pb}$ collision at the laboratory energy of $E_{lab} = 158\text{ AGeV}$ with the K -factor 1.0 (original version uses $\eta = 0.035$) of net protons with the data [5]. It is seen that contribution from parton cluster is negligibly small, thus baryon stopping behavior is fully explained by soft physics (in this case, beam cluster decay) when we chose the K -factor 1.0 at SPS energies. It should be noted that there is no microscopic dynamics in the modeling of the beam cluster formation in the parton cascade model, but it is a simple fit to the data of pp collisions.

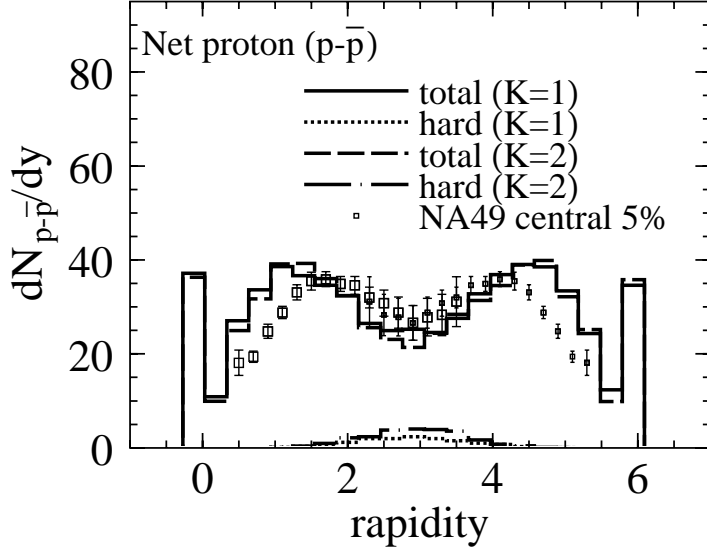


FIG. 2. Parton cascade model calculations of the rapidity distributions of net protons for $\text{Pb} + \text{Pb}$ collision at SPS energy ($E_{lab} = 158\text{ AGeV}$). $K = 1.0$ (solid and dotted lines) and $K = 2.0$ (dashed and dash-dotted lines) are used in this calculation. Dotted and dash-dotted lines corresponds to the contribution from parton cluster decay respectively.

C. Predictions for RHIC

The K -factor dependence of both net proton and charged particle rapidity distribution are studied in Fig. 3. In terms of net proton distribution, there is no strong K -factor dependence. We can see that parton cluster formation and its decay predict almost baryon free at mid-rapidity region regardless of the choice of K -factor, though there are lots of protons and antiprotons at mid-rapidity. We conclude that hard parton scattering plays no role for the baryon stopping within a parton cascade model. However, note that string based model like HIJING/B [9,10] predicts proton rapidity density of 10 and UrQMD predicts [26] 12.5 at mid-rapidity. However, as pointed out in Ref. [23], charged hadron multiplicity is strongly depend on how to chose the leading order correction scheme.

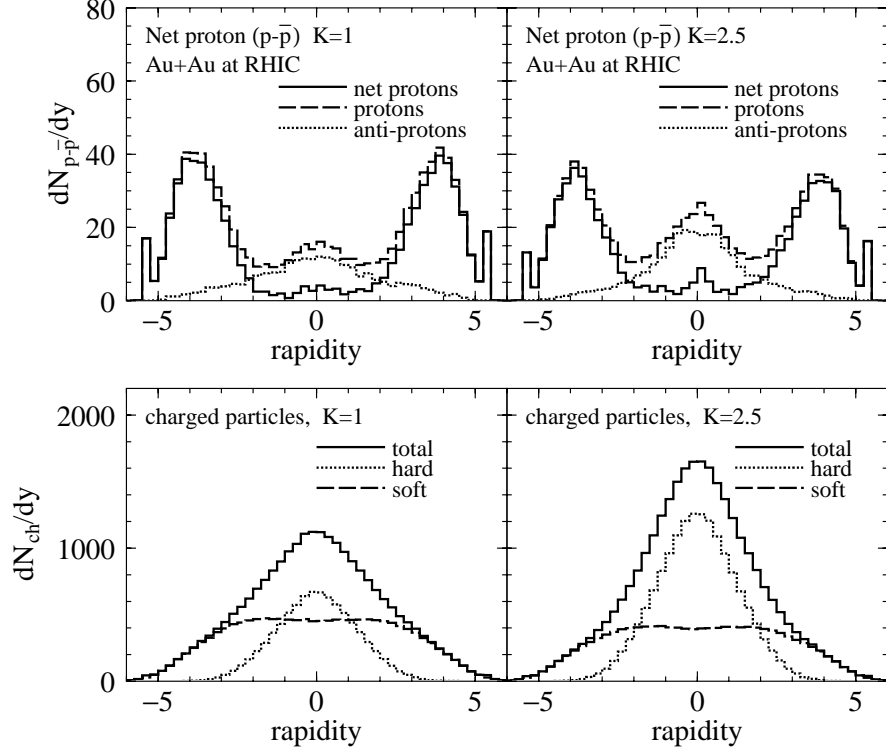


FIG. 3. Parton cascade model calculations of the rapidity distributions of net protons, protons, and anti-protons (upper) and charged particles (lower) for Au + Au collision at $E_{c.m.} = 200$ AGeV for head on collisions.

Fig. 4 displays the net baryon number distributions as a function of rapidity obtained by parton distribution from parton cascade before hadronization with the K -factor of 1 (left) and 2.5 (right). Net baryon number of time-like partons are distributed around mid rapidity region but its contribution are small as consistent with the net proton distribution in Fig. 3.

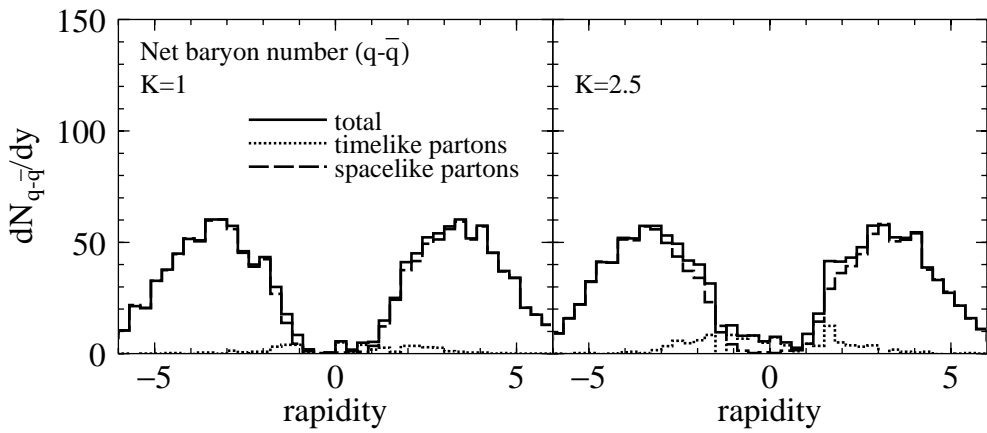


FIG. 4. Rapidity distributions of net baryon number ($q - \bar{q}$) obtained from parton cascade model before hadronization with $K = 1$ (left) and $K = 2.5$ (right) for Au + Au collision at $E_{c.m.} = 200$ AGeV for head on collisions.

IV. SUMMARY

In summary, first, we have checked that different treatments for the inclusion of higher-order pQCD corrections in parton cascade model can fit the elementary $p\bar{p}$ collisions. We have to check other elementary processes to fix the model parameters. We show the net proton rapidity distribution at SPS energies to demonstrate that the beam cluster treats underlying soft physics in the parton cascade model reasonably well for nucleus nucleus collisions. Then, we have calculated the net proton rapidity distribution at RHIC energy as well as charged particle distributions using modified version of parton cascade code VNI in which we newly introduced baryonic parton cluster formation and higher hadronic resonance states from decay of parton and beam cluster. Within a framework of perturbative parton cascading and dynamical hadronization scheme, we predict almost baryon free plasma at RHIC energy. The charged particle rapidity distributions are also studied with the parameter set which are fitted by $p\bar{p}$ collisions. Strong K -factor dependence on the hadron multiplicity is seen as previously being found by Ref. [23]. we can not fix the K -factor from only rapidity and transverse momentum distributions for $p\bar{p}$ collisions.

In this work, we consider only two or three parton coalescence, but in dense parton matter produced in heavy ion collisions, this assumption might be broken down. Inverse processes like hadron conversion to parton such as $C \rightarrow q\bar{q}$ are also ignored which might become important at higher colliding energies.

ACKNOWLEDGMENTS

This work should have been collaborated with Klaus Geiger if he had not had perished in the air crash. I would like to thank Dr. S. A. Bass and Prof. R. S. Longacre for careful reading of this paper and useful comments. I am indebted to S. Ohta for encouragements and useful comments.

- [1] Proceedings of Quark Matter '96, *Nucl. Phys.* **A610**, 1c (1996).
- [2] Proceedings of Quark Matter '97, *Nucl. Phys.* **A638**, 1c (1998).
- [3] Proceedings of Quark Matter '99, *Nucl. Phys.* **A661**, 3c (1999).
- [4] L. Ahle, *et al.*, *Phys. Rev. C* **57**, R466 (1998).
- [5] H. Appelhäuser, *et al.*, (NA49 Collaboration) *Phys. Rev. Lett.* **82**, 2471 (1999).
- [6] S. Jeon and J. Kapusta, *Phys. Rev. C* **56**, 468 (1997).
- [7] K. Werner, *Z. Phys. C* **42**, 85 (1989); *Phys. Rep.* **232**, 87 (1993).
- [8] H. Sorge, *Phys. Rev. C* **52**, 3291 (1995).
- [9] S. E. Vance, M. Gyulassy and X. N. Wang, *Phys. Lett. B* **443**, 1 (1998).
- [10] S. E. Vance and M. Gyulassy, *Phys. Rev. Lett.* **83**, 1735 (1999); e-print: nucl-th/9901009.
- [11] A. Capella, *Phys. Lett. B* **364**, 175 (1995); A. Capella and C. A. Salgado, *Phys. Rev. C* **60**, 054906 (1999).
- [12] S.A. Bass, M. Belkacem, M. Bleicher, M. Brandstetter, L. Bravina, C. Ernst, L. Gerland, M. Hofmann, S. Hofmann, J. Konopka, G. Mao, L. Neise, S. Soff, C. Spieles, H. Weber, L.A. Winckelmann, H. Stöcker, W. Greiner, C. Hartnack, J. Aichelin and N. Amelin, *Prog. Part. Nucl. Phys.* **41**, 225 (1998); nucl-th/9803035.
- [13] X. N. Wang and M. Gyulassy, *Phys. Rev. D* **44**, 3501 (1991).
- [14] X. N. Wang, *Phys. Rep.* **280**, 287 (1997); X. N. Wang and M. Gyulassy, *Comp. Phys. Comm.* **83**, 307 (1994); <http://www-nsdth.lbl.gov/~xnwang/hijing/>.
- [15] K. Geiger, *Phys. Rep.* **258**, 238 (1995); *Comp. Phys. Comm.* **104**, 70 (1997); <http://penguin.phy.bnl.gov/~klaus/>.
- [16] The code can be obtained from <http://quark.phy.bnl.gov/~ynara/vni>.
- [17] K. Geiger and D. K. Srivastava, *Phys. Rev. C* **56**, 2718 (1997); D. K. Srivastava and K. Geiger, *Phys. Lett. B* **422**, 39 (1998). K. Geiger and R. Longacre, *Heavy Ion Phys.* **8**, 41 (1998).
- [18] K. Geiger, *Phys. Rev. D* **50**, 50 (1994); *Phys. Rev. D* **54**, 949 (1996); *Phys. Rev. D* **56**, 2665 (1997).
- [19] K. Geiger, *Phys. Rev. D* **51**, 3669 (1995).
- [20] J. Ellis and K. Geiger, *Phys. Rev. D* **52**, 1500 (1995).
- [21] J. Ellis and K. Geiger, *Phys. Rev. D* **54**, 1967 (1996); J. Ellis and K. Geiger and H. Kowalski, *Phys. Rev. D* **54**, 5443 (1996); J. Ellis and K. Geiger, *Phys. Lett. B* **404**, 230 (1997).
- [22] M. Glueck, E. Reya and A. Vogt, *Z. Phys. C* **67**, 433 (1995).
- [23] S.A.Bass and B.Müller, *Phys. Lett. B* **471**, 108 (1999), nucl-th/9908014.
- [24] UA5 Collaboration, G.J.Alner, *et al.*, *Z. Phys. C* **33**, 1 (1984).

- [25] UA1 Collaboration, C. Albajar, *et al.*, *Nucl. Phys.* **B335**, 261 (1990).
- [26] M. J. Bleicher, *et al.*, e-print: hep-ph/9911420.